KSOE

Journal of Ocean Engineering and Technology 36(4), 217-231, August, 2022
https://doi.org/10.26748/KSOE.2022.023

pISSN 1225-0767
eISSN 2287-6715

Original Research Article

Assessment of Cryogenic Material Properties of R-PUF Used in the CCS of an LNG Carrier

Ha-Cheol Song[1]

[1]*Professor, Department of Naval Architecture and Ocean Engineering, Mokpo National University, Jeonnam, Korea*

KEY WORDS: LNG cargo containment system (LNG CCS), Insulation system, Cryogenic test, Reinforced polyurethane foam (R-PUF), LNG carrier, Secondary barrier

ABSTRACT: *Reinforced polyurethane foam (R-PUF), a material for liquefied natural gas cargo containment systems, is expected to have different mechanical properties depending on its stacking position of foaming as the glass fiber reinforcement of R-PUF sinks inside R-PUF under the influence of gravity. In addition, since R-PUF is not a homogeneous material, it is also expected that the coordinate direction within this material has a great correlation with the mechanical properties. So, this study was conducted to confirm this correlation with the one between the mechanical properties and the stacking position. In particular, in this study, R-PUF of 3 different densities (130, 170, and 210 kg/m^3) was used, and tensile, compression, and shear tests of this material were performed under 5 temperatures. As a result of the tests, it was confirmed that the strength and modulus of elasticity of the material increased as the temperature decreased. Specifically, the strength and modulus of elasticity in the Z direction, which was the lamination direction, tended to be lower than those in the other directions. Finally, the strength and elastic modulus of different specimens of the material found at the bottom of their lamination compared to the specimens with these properties found at positions other than their lamination bottom were evaluated. Further analysis confirmed that as the temperature decreased, hardening of R-PUF occurred, indicating that the strength and modulus of elasticity increased. On the other hand, as the density of R-PUF increased, a sharp increase in strength and elastic modulus of R-PUF was observed.*

1. Introduction

Recently, as part of the response from the international community to global warming, regulations on greenhouse emissions and the marine environment are being strengthened day by day through climate agreements and IMO (International Maritime Organization). As a measure of responding to these environmental regulations, the amount of liquefied natural gas (LNG) used, which can reduce the emission of SOx by 97%, NOx by 80%, and CO_2 by 25%, is rapidly increasing worldwide. Notably, the LNG projects of the world usually consist of LNG carriers, LNG-fueled vessels, and LNG offshore structures. In addition, due to the nature of transporting or storing LNG, LNG cargo holds and fuel tanks must be at a cryogenic temperature of -163°C. So, as shown in Table 1, the interior of the LNG cargo hold consists of the primary barrier; and stainless steel (SUS type), polyurethane foam (PUF), plywood, and adhesives constituting the secondary barrier.

In addition, when the natural frequency of the cargo hold of an LNG carrier is the same as that of the ship, the sloshing impact load of LPG amplifies, which is dangerous. Therefore, to ensure the structural safety of the cargo hold, impact, compression, and tensile tests on reinforced polyurethane foam (R-PUF) should be performed under cryogenic conditions where R-PUF specimens manufactured according to the recommendations of GTT (Gaztransport & Technigaz) are placed in an environment similar to the one inside the cargo hold (Han et al., 2010).

In addition, the effect of repeated impact on the mechanical performance of glass fiber-reinforced PUF was analyzed as repeated compressive loads were generated in this PUF due to the effect of the sloshing impact load and their understanding was important (Kim et

Table 1 A MARK Ⅲ type LNG cargo insulation material specification

Primary barrier	Corrugated SUS 304L 1.2 mm
Primary insulation	Plywood covered reinforced PUF (100 mm)
Secondary barrier	Glued triplex membrane
Secondary insulation	Plywood covered reinforced PUF (170 mm)

Received 19 July 2022, revised 8 August 2022, accepted 10 August 2022
Corresponding author Ha-Cheol Song: +82-61-450-2767, hcsong@mnu.ac.kr

ⓒ 2022, The Korean Society of Ocean Engineers
This is an open access article distributed under the terms of the creative commons attribution non-commercial license (http://creativecommons.org/licenses/by-nc/4.0) which permits unrestricted non-commercial use, distribution, and reproduction in any medium, provided the original work is properly cited.

al., 2019a). Consequently, it was confirmed that the glass fiber-reinforced PUF exhibited a sharp decrease in its impact resistance and compression according to the repeated impact conditions when impact energy above a critical level was continuously applied.

Next, an isotropic Frank-Brockman type elastic-isoplastic model was introduced to simulate the compression behavior of an LNG cargo hold, considering the effects of cryogenic temperatures and strain rate (Lee et al., 2015). This simulation was performed in Abaqus UMAT, one of the finite element analysis codes. In particular, the elastic deformation according to the temperature and strain rate of R-PUF subjected to a compressive load was simulated. Finally, the simulation results were compared with the results of a series of compression tests on the material to verify the model.

LNG cargo holds are subjected to various temperatures, from room to cryogenic temperature So, an experimental basis for evaluating the mechanical performance of R-PUF at cryogenic temperatures was developed by closely analyzing the compression properties of R-PUF (Park et al., 2014). In particular, the compression characteristics at temperatures of 296, 223, 163, and 110 K were analyzed and evaluated so that the phenomenological temperature-dependent insulation properties of R-PUF could be identified. Finally, based on the analysis, the experimental basis necessary for the evaluation of the applicability of R-PUF as a cargo hold insulation material of an LNG carrier was formed.

The cryogenic heat transfer characteristics and thermoelastic behavior of R-PUF were examined by Jang et al. (2013) by performing a numerical analysis of this material using a general-purpose finite element analysis code. In particular, a numerical analysis based on forced convection theory was performed to understand the cryogenic heat transfer characteristics. Additionally, a comparative review of the cryogenic heat transfer and thermoelastic deformation characteristics according to the density change of R-PUF evaluated by numerical and experimental methods, respectively, was performed.

Kim et al. (2019b) improved the performance of existing single-reinforced R-PUF by adding glass bubble and silica aerogel into the R-PUF and analyzed the thermal insulation performance and mechanical properties of the resulting R-PUF. Specifically, the physical properties of the resulting R-PUF according to the weight ratio of addition in this R-PUF were analyzed. In addition, the effect of ultrasonic dispersion of the added materials on the inner cell structure of R-PUF was investigated. Finally, mechanical strength, dynamic impact, and quasi-static compression tests on the R-PUF added with glass bubble and silica aerogel were performed at cryogenic and room temperatures.

Further, improvement in the mechanical and thermal performances of R-PUF used in existing LNG cargo hold insulation systems was achieved by Ahn et al. (2018) with the addition of glass bubbles into R-PUF in various weight ratios and the mechanical and thermal properties of the resulting R-PUF were evaluated under various temperatures. Consequently, a performance change of R-PUF was observed according to the amount of glass bubble added. In particular, the mechanical strength of the R-PUF added with glass bubbles found by conducting compression tests on this material under various temperatures (-163, -100, -40, and 20°C) resulted in this observation. Finally, for comparing the thermal insulation performances of R-PUFs with different glass bubble additions, the thermal conductivity of glass bubble-added R-PUFs was measured.

In a different approach, instead of glass fiber, Kevlar aramid fiber with excellent mechanical strength and thermal performance was added to PUF, and the effect of this addition on the cell structure of PUF was analyzed by Oh et al. (2018). And as a material test, a compression test at different temperatures was performed on the Kevlar aramid fiber-added PUF. Notably, aramid fibers are stronger than steel and have high heat resistance, high elasticity, and excellent flame retardancy. Meanwhile, changes in the properties of the cell structure were observed depending on the amount of fiber added.

The extensive material behavior and failure characteristics of PUF and R-PUF at low and cryogenic temperatures and under static compressive loads were studied experimentally by Park et al. (2016). In addition, the micro-structural cellular variation of three types of PUF materials according to temperature changes was identified, and a micromechanical approach was introduced to describe the failure characteristics of PUF.

Next, the behavior of R-PUF under repeated compression and creep loads was analyzed under room to cryogenic temperatures by Denay et al. (2013). The thermal and mechanical damages of R-PUF were also investigated as part of the analysis. Finally, creep and cyclic tests aiming at finding how far viscoelasticity and/or damage contribute(s) to the deformation of R-PUF were conducted.

However, although various studies have been conducted on R-PUF, there is no study on the correlation of mechanical properties according to the stacking location and coordinate direction of R-PUF. So, research on this correlation is necessary.

Therefore, in this study, R-PUF with three different densities (130, 170, and 210 kg/m^3) was used, and specific stacking positions (bottom, middle, and upper) and coordinate directions (X, Y, and Z in Fig. 1) were chosen to study the R-PUF at room temperature. In particular, tensile, compression, and shear tests were performed on the R-PUF. Further, in a low-temperature environment (-20, -70, -120, and -170 °C), specimens of R-PUF with middle stacking position and three different coordinate directions (X, Y, and Z) were considered, and the mechanical properties of the samples were studied by performing tensile, compression, and shear tests. Notably, a cryogenic chamber was manufactured, and liquid nitrogen (LN2) was used as its refrigerant for this study. Also, considering the thermal conductivity of R-PUF, each test was performed after maintaining the R-PUF at the target temperature for 3 h or more.

2. Test Specimen

2.1 R-PUF

R-PUF is a composite material made by laminating high-density

Table 2 Specified and average measured densities of R-PUF specimens

Specified density (kg/m^3)	Stacking position	Measured density in X direction[1] (kg/m^3)	Measured density in Y direction[1] (kg/m^3)	Measured density in Z direction[1] (kg/m^3)
130	Upper	123.89 (0.45)	127.40 (1.10)	128.83 (1.20)
	Middle	119.89 (0.54)	121.00 (0.38)	122.09 (3.08)
	Bottom	128.36 (0.35)	128.67 (0.36)	130.71 (0.69)
170	Middle	180.91 (1.13)	180.74 (1.65)	175.85 (1.31)
210	Middle	220.85 (1.11)	219.58 (1.90)	216.62 (1.74)

[1] Values within the brackets denote the standard deviation of the corresponding density.

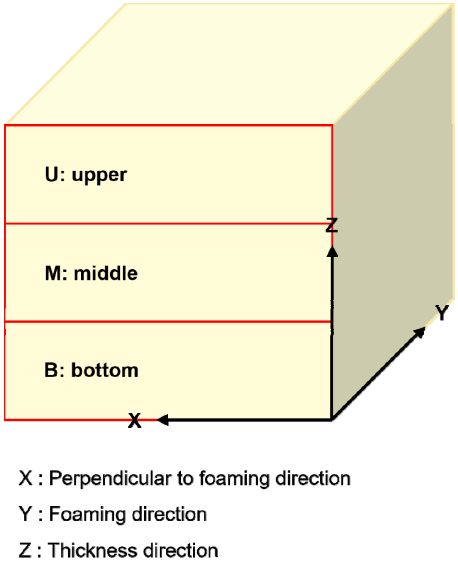

Fig. 1 R-PUF coordinates and stacking position definition

polyurethane foam and glass fiber. R-PUF is currently used as a Mark-Ⅲ type insulation material and has excellent mechanical and insulation performances. In addition, R-PUF can be produced with various densities depending on its glass fiber content. Here, the R-PUF used for this study was obtained from Hankuk Carbon and manufactured by Hyundai Heavy Industries. The R-PUF specimen coordinates and stacking position definition are given in Fig. 1.

Before the tests, the density of all specimens was thoroughly inspected, and it was found that the density had a variation of 10% or less with respect to the specified density of the specimen material. Table 2 gives the density from the inspection.

2.2 Tensile Test Specimen

The specimen for the tensile test of R-PUF was prepared according to the ASTM D1623-03 standard (the standard for testing the tensile and tensile adhesion properties of rigid cellular plastics). The dimensions of the specimen are given in Fig. 2.

2.3 Compression Test Specimen

The specimen for the compression test of R-PUF was prepared according to the ISO 844 standard. Fig. 3 shows the dimensions of the specimen that have a ±1 mm variation.The dimensions of the specimen are given in Fig. 3.

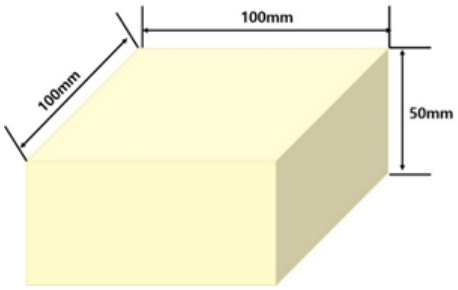

Fig. 3 R-PUF compression test specimen dimensions

2.4 Shear Test Specimen

The specimen for the shear test of R-PUF was prepared according to the ISO 1922 standard. The dimensions of the specimen are given in Fig. 4.

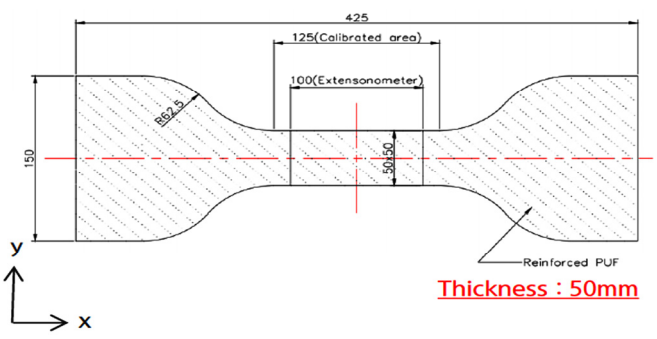

(a) Specimen dimensions on the XY plane

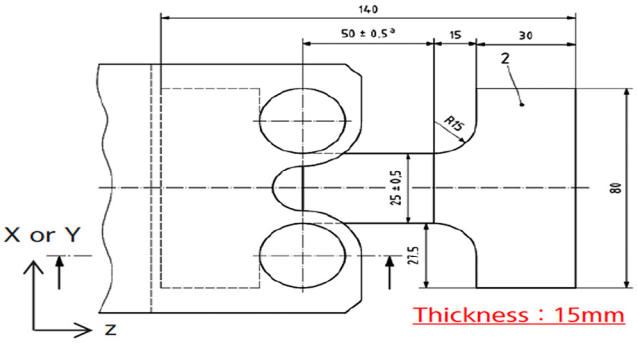

(b) Z-directional specimen dimensions

Fig. 2 R-PUF tensile test specimen dimensions

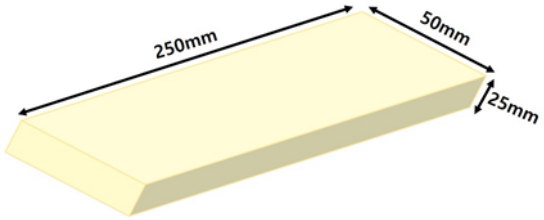

Fig. 4 R-PUF shear test specimen dimensions

3. Experiments

3.1 Test Facility

The cryogenic tests of the study were performed using a cryogenic chamber and 50 and 250 kN MTS universal testing machines. In addition, PT-100 temperature sensors were used inside the chamber to measure the temperature immediately next to the specimen and in the upper and lower parts of the chamber to ensure a stable temperature inside the chamber. R-PUF is a special material that minimizes heat transfer as an insulator, so pre-cooling is required for more than 3 hours. Fig. 5 shows the universal testing machines used in this study.

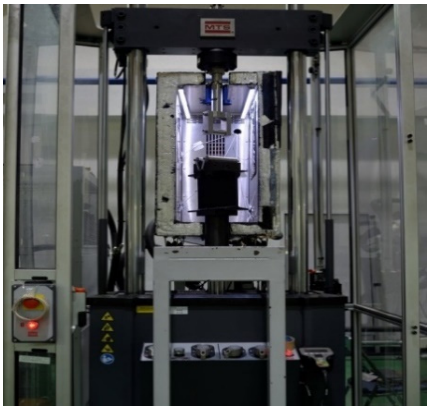

(a) 50 kN MTS universal testing machine used in the study

(b) 250 kN MTS universal testing machineused used in the study

Fig. 5 50 and 250 kN MTS universal testing machine used in the study

3.2 Cooling Time and Methodology

For the cryogenic test, LN2 was injected into the cryogenic chamber to maintain a cryogenic state inside the chamber. Temperature sensors were then attached to the upper/lower parts of the chamber to check the temperature in these positions in real time. Additionally, for a uniform temperature distribution of the specimen, a temperature sensor was attached to the specimen to check the target temperature (for maintaining this temperature for 3 h before conducting the test). So, the temperature history curves at various points are given in Fig. 6. Since the specimen and the plate jig used for holding the specimen during the test usually contract while reaching the target temperature, zero-offset of the linear variable differential transformer of the test setup (used for linear distance measurements) should be corrected according to the contraction before starting the test. The related schematic specimen shrinkage control is shown in Fig. 7.

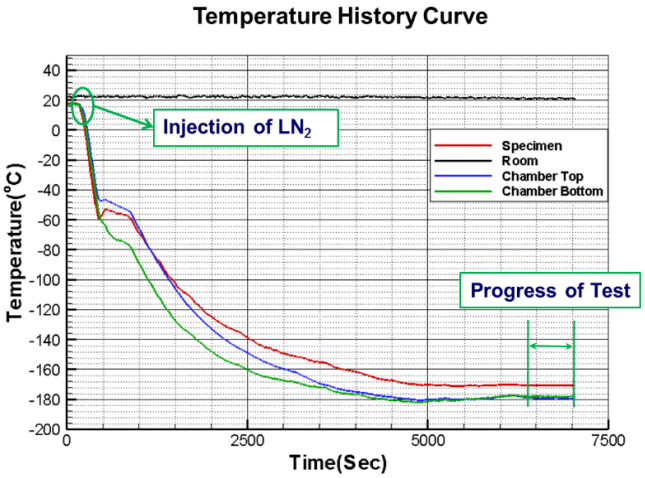

Fig. 6 Temperature history curves at various points during a typical test on R-PUF of this study

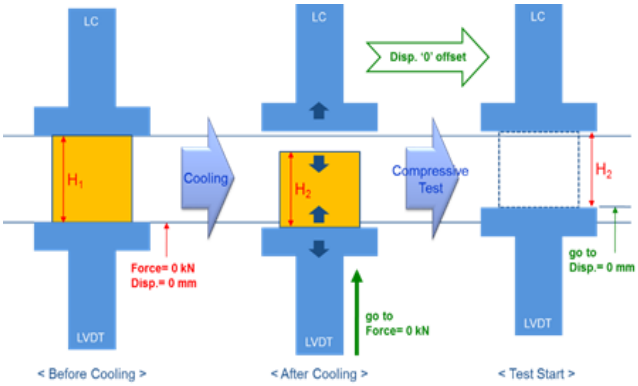

Fig. 7 Schematic R-PUF specimen shrinkage control during a cryogenic test of this study

3.3 Tensile Test Methodology

The tensile test of R-PUF was conducted at cryogenic temperature, and the ultimate tensile strength and tensile Young's modulus of R-PUF were found from the force-deformation curve obtained from the test. The tensile test setup is shown in Fig. 8.

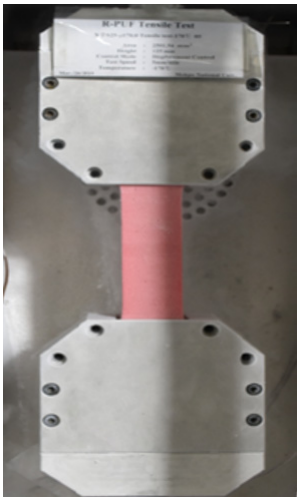

(a) XY planar view of the setup showing the R-PUF specimen

(b) Z-directional view of the setup showing the R-PUF specimen

Fig. 8 Experimental setup for the tensile test of R-PUF

Mathematically, the elongation (e) of a specimen during the tensile test was expressed as a percentage of the original sample length as,

$$e = \frac{\Delta L_o}{L_o} \times 100 \tag{1}$$

where, L_o and ΔL_o were the original distance between the marks on the specimen and the increase in the distance between these marks corresponding to a specified force increment, respectively.

Further, the ultimate stress ($\sigma_{\max}$) inside the specimen was expressed as,

$$\sigma_{\max} = \frac{F_{\max}}{b \times h} \tag{2}$$

where, $F_{\max}$, b, and h were the maximum force applied to the specimen during the test, the original width of the narrow part of the specimen, and the original thickness of the narrow part of the specimen, respectively.

In addition, the tensile Young's modulus of R-PUF (E) was expressed as,

$$E = \frac{\sigma(\epsilon)}{\epsilon} = \frac{F/A}{\Delta L/L_o} = \frac{FL_o}{A\Delta L} \tag{3}$$

where, E, F, A, ΔL, and L_o were the force applied on the specimen, area of cross-section of the specimen perpendicular to the direction of the applied force, an increase in the distance between the marks on the specimen corresponding to a specified force increment, and the original distance between these marks, respectively.

3.4 Compression Test Methodology

The compression test on R-PUF was performed at room/cryogenic temperature, and the compressive ultimate strength and compressive Young's modulus of R-PUF were found from the stress-strain curve obtained from the test. For the test, first, an R-PUF sample was placed between the plates of the compression tester (one of the variants in the universal testing machine), and the sample center was aligned with the plates. Subsequently, the moving plate of the tester was moved at a constant speed, compressing the specimen. Generally, if possible, the test speed should be 10% of the measured specimen thickness before compression/min. So, under this condition on the test speed, the sample was compressed, and the ultimate compressive strength and ultimate compressive strength at 10% relative strain of the sample were measured. The experimental setup for the compression test is shown in Fig. 9.

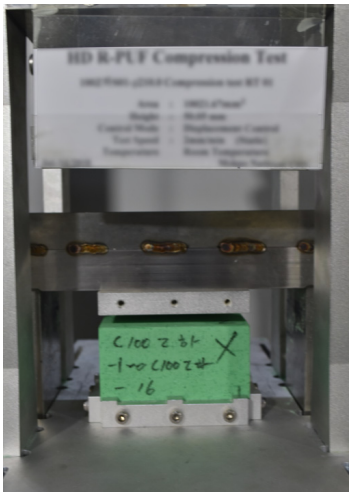

Fig. 9 Experimental setup for the compression test of R-PUF

The ultimate compressive strength (σ_m) inside the sample was obtained by dividing the maximum compressive load on the sample (F_m) by the initial cross-sectional area of the sample (A) when the elongation of the sample was 10% or more as,

$$\sigma_m = \frac{F_m}{A} \tag{4}$$

3.5 Shear Test Methodology

The R-PUF shear test was performed on the XY, YZ, and ZX planes and certain specified directions. In particular, the test was performed on an R-PUF specimen with a density of 130 kg/m^3 at room temperature for each stacking position (upper, middle, and bottom). In addition, the test temperatures were -20, -70, -120, and -170°C, and a displacement control methodology was used for the test. The experimental setup for the shear test of R-PUF is shown in Fig. 10.

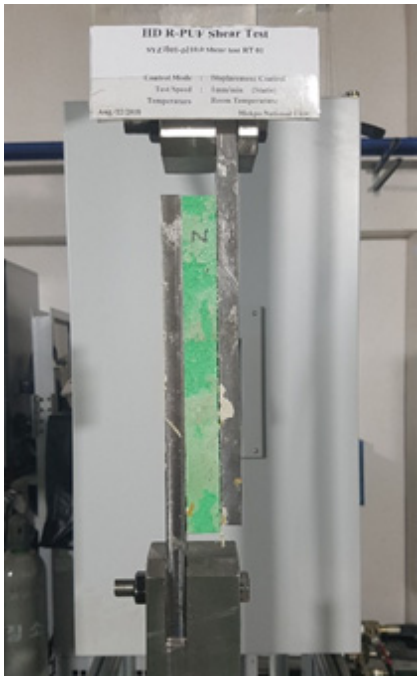

Fig. 10 Experimental setup for the shear test of R-PUF

Meanwhile, the shear stress (τ) within the sample was expressed as,

$$\tau = \frac{1{,}000 \times F_m}{b \times l} \tag{5}$$

where, G, l, and b were the maximum force applied onto the specimen during the test (N), the original length of the specimen, and the original width of the specimen, respectively.

Likewise, the shear modulus of R-PUF (G) was expressed as,

$$G = \frac{1{,}000 \times \delta \times \theta}{b \times l} \tag{6}$$

where, δ and θ were the specimen thickness and the slope of the linear portion of the force-strain curve.

3.6 Test Condition

As mentioned before, it was expected that differences in strength and Young's modulus would occur for each stacking position of R-PUF, so the tests were performed under each stacking position at room temperature. However, when the stacking position was not specifically stated, it meant the default middle stacking position. Further, reliable results of each test were obtained by conducting the test under the same conditions 5 times to obtain valid/reliable test data.

Importantly, in the shear test of R-PUF, when the R-PUF density was 170 kg/m^3 or more, a fracture occurred at the bonding surface of the R-PUF specimen and the plate jig, so the test was performed with a density of only 130 kg/m^3. Finally, Table 3 shows the number and types of tests conducted.

Table 3 The number and types of tests conducted in this study (X, Y, Z, XY, YZ,, ZX, U, M, and B in the table denote the coordinate directions, coordinate planes, and stacking positions, respectively, in/on/at which the measurements of this test were made)

Material (Specified density)	Temperature (°C)	Tensile test									Compression test									Shear test								
		X			Y			Z			X			Y			Z			XY			YZ			ZX		
		U	M	B	U	M	B	U	M	B	U	M	B	U	M	B	U	M	B	U	M	B	U	M	B	U	M	B
	20	5	5	5	5	5	5	5	5	5	5	5	5	5	5	5	5	5	5	5	5	5	5	5	5	5	5	5
R-PUF (130 kg/m^3)	-20	5			5			5			5			5			5			5			5			5		
	-70	5			5			5			5			5			5			5			5			5		
	-120	5			5			5			5			5			5			5			5			5		
	-170	5			5			5			5			5			5			5			5			5		
R-PUF (170 kg/m^3)	20	5			5			5			5			5			5			·			·			·		
	-20	5			5			5			5			5			5			·			·			·		
	-70	5			5			5			5			5			5			·			·			·		
	-120	5			5			5			5			5			5			·			·			·		
	-170	5			5			5			5			5			5			·			·			·		
R-PUF (210 kg/m^3)	20	5			5			5			5			5			5			·			·			·		
	-20	5			5			5			5			5			5			·			·			·		
	-70	5			5			5			5			5			5			·			·			·		
	-120	5			5			5			5			5			5			·			·			·		
	-170	5			5			5			5			5			5			·			·			·		

4. Test Results

4.1 Tensile Test

Since the ultimate tensile strength and tensile modulus are expected to be different depending on the PUF stacking direction, the test was conducted in a total of 9 cases: upper, middle, and bottom with a density of 130 kg/m^3 in each direction. In addition, since ultimate tensile strength and tensile modulus are expected to be different for each temperature, each density (130, 170, and 210 kg/m^3) is tested at 20, -20, -70, -120, and -170°C. A total of 15 cases were performed.

As shown in Fig. 11 and Fig. 12, differences in ultimate tensile strength and tensile modulus occurred depending on the foaming location and foaming direction.

In the case of the X-direction specimen, the ultimate tensile strength and tensile modulus of the bottom tended to be high. ultimate tensile strength increased by about 21% compared to the upper and 14.7% compared to the middle. The young's modulus increased by about 15.8% compared to the upper, and increased by about 15.6% compared to the middle.

In the case of the Y-direction specimen, as in the X-direction, the ultimate tensile strength and tensile modulus of the bottom tended to be high. ultimate tensile strength increased by about 26.2% compared to the upper and 18.1% compared to the middle. The tensile modulus increased by about 20.7% compared to the upper, and increased by about 18.6% compared to the middle.

In the case of the Z-direction specimen, the ultimate tensile strength and tensile modulus of the middle part were high, unlike the specimens in the X and Y directions. ultimate tensile strength increased by about 37.9% compared to the upper and by 38.6% compared to the bottom. The tensile modulus increased by 152.9% compared to the upper and 133.6% compared to the bottom.

Also, the difference in ultimate tensile strength and tensile modulus occurred according to the direction of foaming.

In the case of the upper part, the ultimate tensile strength and tensile modulus in the Z-direction tended to be low. The ultimate tensile strength decreased by 54.7% compared to the X direction and

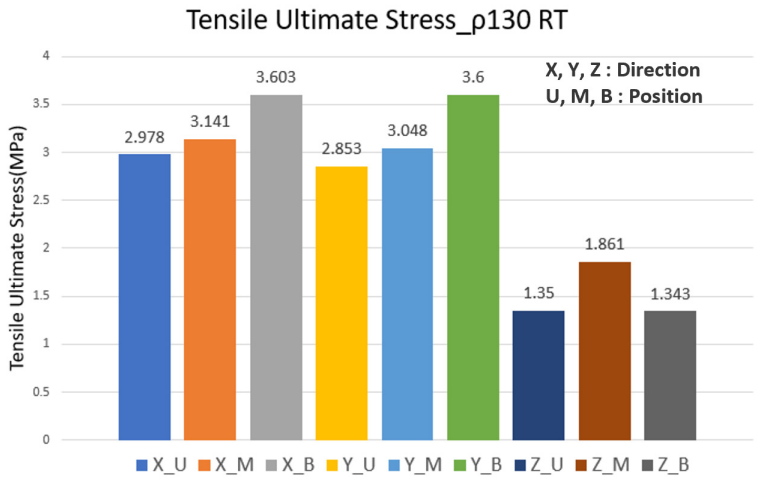

Fig. 11 Ultimate tensile strength of R-PUF by stacking position and coordinate direction for an R-PUF density of 130 kg/m^3 at room temperature

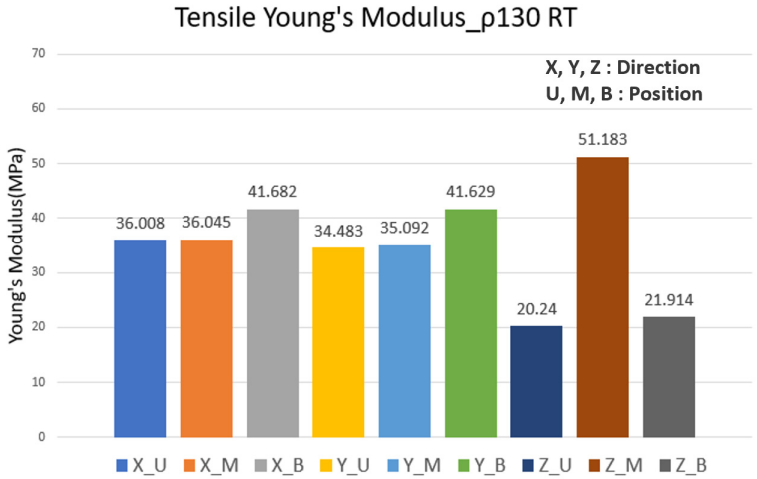

Fig. 12 Tensile Young's modulus of R-PUF by stacking position and coordinate direction for an R-PUF density of 130 kg/m^3 at room temperature

Table 4 R-PUF tensile test results

Material (Specified density)	Temperature (°C)	Ultimate tensile strength (MPa)[1]			Tensile Young's modulus (MPa)[1]		
		In X direction	In Y direction	In Z direction	In X direction	In Y direction	In Z direction
R-PUF (130 kg/m^3)	20	3.141 (0.067)	3.048 (0.151)	1.861 (0.384)	36.045 (1.546)	35.092 (1.146)	51.183 (5.072)
	-20	3.508 (0.252)	3.477 (0.358)	3.213 (0.496)	41.983 (1.935)	41.244 (2.202)	64.368 (2.101)
	-70	3.643 (0.229)	3.752 (0.168)	2.543 (0.300)	45.077 (3.333)	46.442 (3.387)	47.915 (10.33)
	-120	3.653 (0.484)	3.760 (0.449)	2.394 (0.147)	50.804 (3.151)	50.933 (2.944)	43.774 (5.732)
	-170	3.299 (0.213)	3.123 (0.404)	1.970 (0.315)	54.198 (2.548)	51.149 (3.143)	49.161 (2.913)
R-PUF (170 kg/m^3)	20	5.469 (0.472)	5.384 (0.350)	1.888 (0.051)	73.914 (3.291)	73.256 (5.601)	34.243 (0.866)
	-20	5.670 (0.277)	5.595 (0.479)	2.657 (0.059)	72.700 (3.522)	73.721 (3.956)	40.680 (1.160)
	-70	5.928 (0.623)	6.007 (0.689)	2.900 (0.117)	80.100 (6.104)	80.576 (4.098)	47.305 (0.403)
	-120	5.938 (0.429)	5.897 (0.478)	2.667 (0.157)	94.649 (4.964)	93.315 (4.293)	60.284 (0.839)
	-170	5.663 (0.560)	5.286 (0.952)	2.284 (0.106)	96.177 (4.995)	92.010 (9.342)	75.852 (2.751)
R-PUF (210 kg/m^3)	20	7.363 (0.460)	6.451 (0.692)	2.485 (0.147)	100.109 (3.62)	90.787 (5.929)	48.509 (2.650)
	-20	7.552 (0.726)	7.076 (0.593)	3.281 (0.138)	104.801 (6.96)	97.058 (6.363)	56.031 (0.864)
	-70	8.094 (0.832)	7.585 (1.103)	3.644 (0.117)	113.708 (5.77)	108.761 (7.070)	66.144 (1.464)
	-120	8.370 (0.893)	7.492 (0.432)	3.409 (0.177)	123.372 (5.19)	119.250 (2.910)	85.776 (0.873)
	-170	7.806 (0.530)	7.639 (0.480)	3.236 (0.256)	135.712 (5.18)	134.562 (4.390)	105.526 (1.250)

[1] Values within the brackets denote the standard deviation of the corresponding ultimate tensile strength/tensile Young's modulus.

decreased by 52.7% compared to the Y direction. The tensile modulus decreased by 43.8% compared to the X direction and 41.3% compared to the Y direction.

In the case of the middle part, the ultimate tensile strength in the Z direction showed a tendency to decrease, and the tensile modulus showed a tendency to increase. The ultimate tensile strength decreased by 40.8% compared to the X direction and decreased by 38.9% compared to the Y direction. The tensile modulus increased by 42% compared to the X direction and 45.9% compared to the Y direction.

In the case of the bottom part, the ultimate tensile strength and tensile modulus in the Z direction tended to be low. The ultimate tensile strength decreased by 62.7% compared to the X direction and 62.7% compared to the Y direction. The tensile modulus decreased by 47.4% compared to the X direction and 47.4% compared to the Y direction.

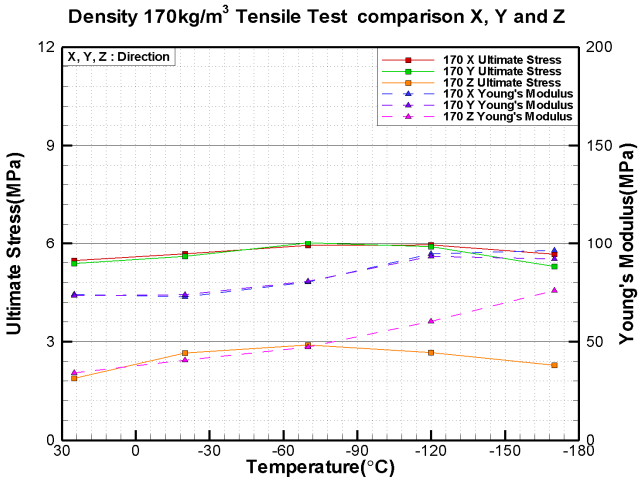

Fig. 14 Density 170 kg/m^3 tensile test comparison X, Y and Z

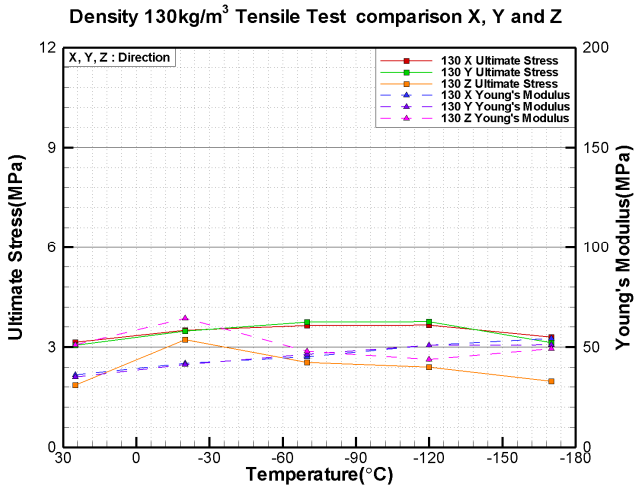

Fig. 13 Density 130 kg/m^3 tensile test comparison X, Y and Z

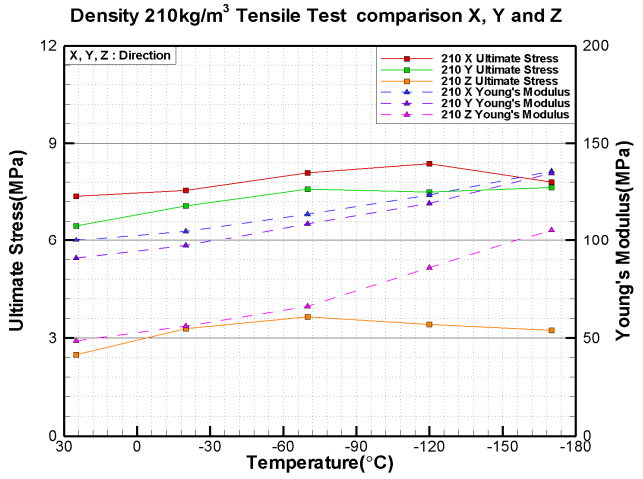

Fig. 15 Density 210 kg/m^3 tensile test comparison X, Y and Z

As shown in Table 4 and Figs. 13–15, it can be seen that the mechanical properties change according to the temperature. As the temperature decreases, the ultimate tensile strength and tensile modulus increase, but show a tendency to decrease again when a certain temperature critical point is exceeded. The standard deviation of all data can be found in Table 4.

4.2 Compression Test

Since the ultimate stress and compressive modulus are expected to be different depending on the PUF stacking direction, the test was conducted in a total of 9 cases: upper, middle, and bottom with a density of 130 kg/m^3 in each direction. In addition, since ultimate stress and compressive modulus are expected to be different for each temperature, each density (130, 170, and 210 kg/m^3) is tested at 20, -20, -70, -120, and -170°C. A total of 15 cases were performed.

As shown in Fig. 16 and Fig. 17, differences in compressive ultimate stress and compressive modulus occurred depending on the foaming location and foaming direction.

In the case of the X-direction specimen, the compressive ultimate stress and compressive modulus of the bottom tended to be high. Compressive ultimate stress increased by about 17.1% compared to the upper and 17.8% compared to the middle. The compressive modulus increased by about 32.4% compared to the upper, and increased by about 31.9% compared to the middle.

In the case of the Y-direction specimen, as in the X-direction, the compressive ultimate stress and compressive modulus of the bottom tended to be high. Compressive ultimate stress increased by about 5.5% compared to the upper and 13.7% compared to the middle. The compressive modulus increased by about 3.3% compared to the upper, and increased by about 13.6% compared to the middle.

In the case of the Z-direction specimen, unlike the specimens in the X and Y directions, there was no significant difference in compressive ultimate stress, and the compressive modulus increased slightly. The compressive ultimate stress decreased by about 0.1% compared to the upper and increased by about 10.1% compared to the middle. The compressive modulus increased by 6.1% compared to the upper and

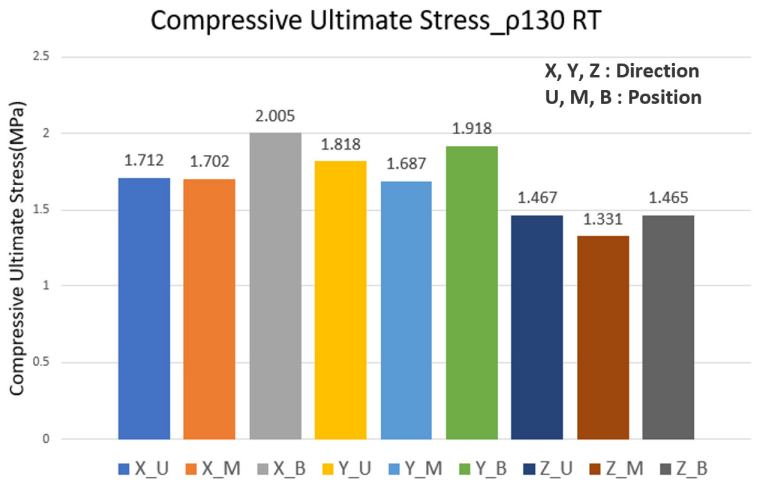

Fig. 16 Ultimate compressive strength of R-PUF by stacking position and coordinate direction for an R-PUF density of 130 kg/m^3 at room temperature

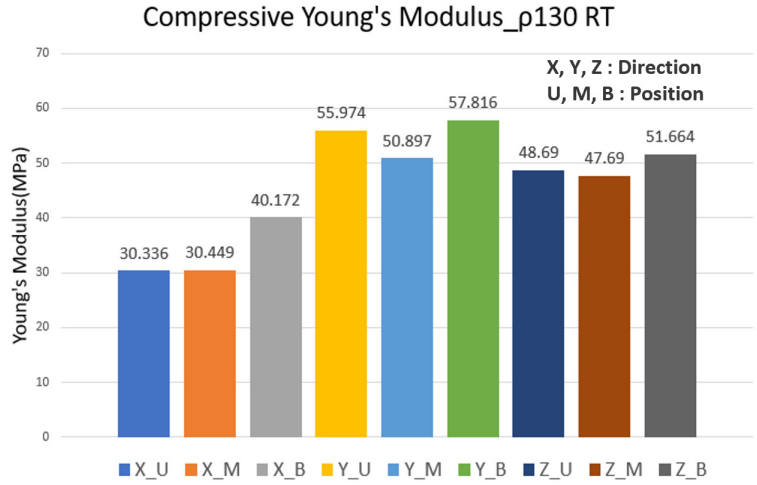

Fig. 17 Compressive Young's modulus of R-PUF by stacking position and coordinate direction for an R-PUF density of 130 kg/m^3 at room temperature

Table 5 R-PUF compressive test results

Material (Specified density)	Temperature (°C)	Ultimate compressive strength (MPa)[1]			Compressive Young's modulus (MPa)[1]		
		In X direction	In Y direction	In Z direction	In X direction	In Y direction	In Z direction
R-PUF (130 kg/m^3)	20	1.702 (0.022)	1.687 (0.015)	1.331 (0.039)	30.449 (1.461)	50.897 (0.379)	47.69 (0.835)
	-20	2.096 (0.071)	2.324 (0.170)	1.714 (0.082)	62.456 (2.240)	73.299 (8.262)	62.407 (0.844)
	-70	2.983 (0.034)	2.843 (0.196)	2.167 (0.117)	86.592 (1.123)	83.607 (6.235)	72.730 (3.417)
	-120	2.924 (0.193)	3.165 (0.115)	2.671 (0.079)	70.173 (9.656)	80.605 (14.89)	76.744 (10.18)
	-170	3.177 (0.064)	3.155 (0.230)	3.038 (0.145)	68.880 (10.93)	79.315 (5.239)	81.649 (8.060)
R-PUF (170 kg/m^3)	20	3.532 (0.092)	3.419 (0.015)	2.299 (0.023)	99.106 (3.409)	101.108 (1.410)	59.951 (0.385)
	-20	4.697 (0.068)	4.439 (0.125)	2.975 (0.050)	143.328 (2.500)	132.611 (2.780)	90.833 (1.110)
	-70	6.162 (0.104)	6.095 (0.173)	4.194 (0.175)	180.557 (1.250)	175.580 (3.240)	114.333 (5.730)
	-120	7.112 (0.074)	7.457 (0.022)	5.454 (0.024)	186.589 (0.980)	197.240 (1.870)	144.976 (1.130)
	-170	8.487 (0.084)	7.587 (0.148)	6.165 (0.065)	211.610 (1.770)	201.538 (2.630)	166.462 (1.870)
R-PUF (210 kg/m^3)	20	5.503 (0.026)	5.590 (0.080)	3.227 (0.022)	93.085 (0.598)	96.229 (0.993)	72.392 (0.828)
	-20	6.926 (0.057)	7.065 (0.083)	4.345 (0.033)	200.401 (1.970)	204.235 (2.540)	133.501 (1.360)
	-70	8.945 (0.115)	6.110 (0.165)	4.289 (0.063)	224.442 (2.980)	175.049 (2.930)	117.914 (2.220)
	-120	11.196 (0.147)	11.325 (0.098)	7.846 (0.061)	241.062 (1.920)	254.826 (3.270)	181.368 (1.810)
	-170	12.374 (0.137)	12.711 (0.180)	8.785 (0.161)	275.146 (0.260)	274.495 (2.550)	213.265 (3.900)

[1] Values inside the brackets denote the standard deviation of the corresponding ultimate compressive strength/compressive Young's modulus.

8.3% compared to the middle.

Also, the difference in compressive ultimate stress and compressive modulus occurred according to the direction of foaming.

In the case of the upper part specimen, the compressive ultimate stress of the Z-direction specimen showed a tendency to be low. The compressive modulus of the specimen in the X direction showed a tendency to be low. The compressive ultimate stress decreased by 14.3% compared to the X direction and decreased by 19.3% compared to the Y direction. The compressive modulus decreased by 45.8% compared to the Y direction and 37.7% compared to the Z direction.

In the case of the middle part specimen, the compressive ultimate stress of the Z-direction specimen showed a tendency to be low as in the upper part. As for the compressive modulus, the specimen in the X direction showed a low tendency. The compressive ultimate stress decreased by 21.8% compared to the X direction and decreased by 21.1% compared to the Y direction. The compressive modulus decreased by 40.2% compared to the Y direction and 36.2% compared to the Z direction.

In the case of the bottom part specimen, the compressive ultimate stress of the Z-direction specimen showed a tendency to be low. As for the compressive modulus, the specimen in the X direction showed a low tendency. The compressive ultimate stress decreased by 26.9% compared to the X direction and decreased by 23.6% compared to the Y direction. The compressive modulus decreased by 30.5% compared to the Y direction and 22.2% compared to the Z direction.

As shown in Table 5 and Figs. 18–20, it can be seen that the mechanical properties change according to the temperature. As the temperature decreased, the compressive ultimate stress and compressive modulus increased, and unlike the tensile test results, there was no tendency to decrease as the temperature exceeded a

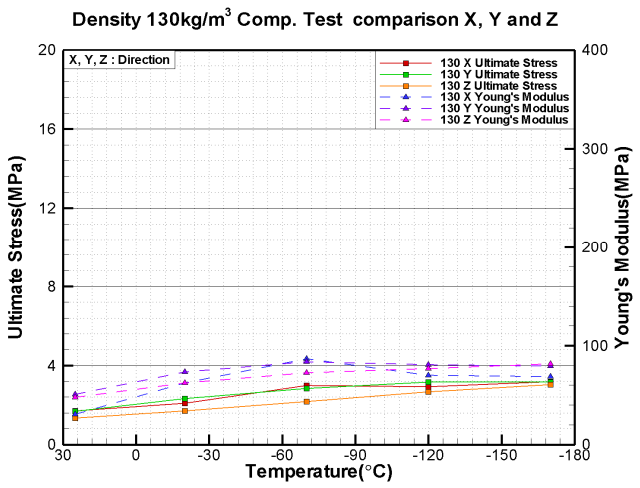

Fig. 18 Density 130kg/m^3 comp. test comparison X, Y and Z

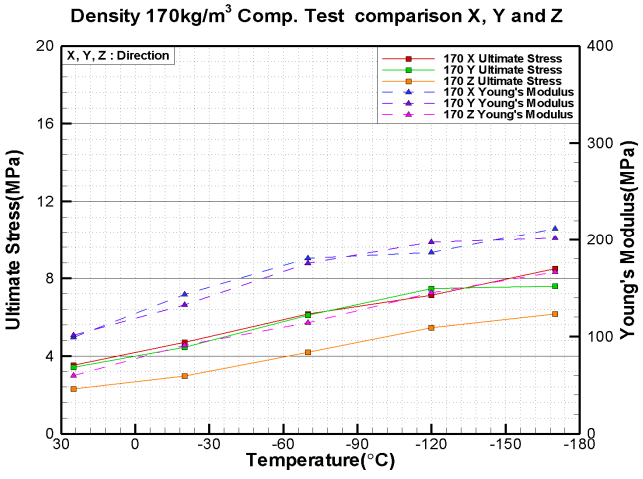

Fig. 19 Density 170kg/m^3 comp. test comparison X, Y and Z

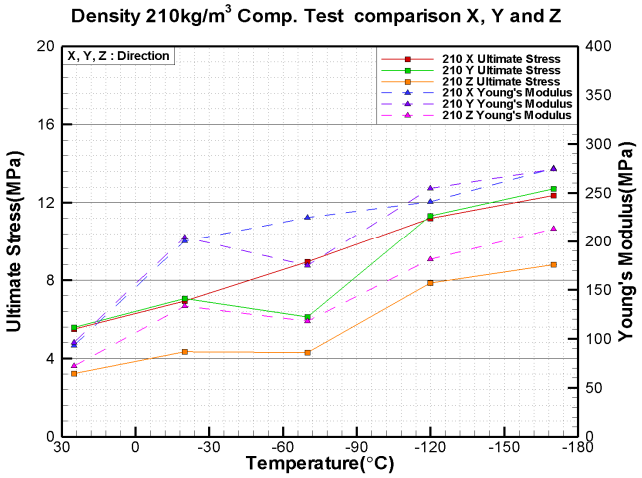

Fig. 20 Density 210kg/m^3 comp. test comparison X, Y and Z

specific temperature critical point. The standard deviation of all data can be found in Table 5.

4.3 Shear Test

The shear test was performed only at a density of 130 kg/m3 because the adhesive broke at densities of 170 and 210 kg/m^3, and the shear test was based on the XY, YZ, and ZX directions. In addition, the test for each foaming position was performed at room temperature. Test temperature conditions were carried out at room temperature, -20, -70, -120, and -170°C. The control mode used displacement control.

As shown in Fig. 21 and Fig. 22, the shear ultimate strength and shear modulus were different depending on the foaming location and foaming direction.

In the case of the XY direction specimen, the shear ultimate strength and shear modulus of the bottom tended to be high. The shear ultimate strength increased by about 8.5% compared to the upper and 11% compared to the middle. The shear modulus increased by about 4.9% compared to the upper and 18.5% compared to the middle.

In the case of the specimen in the YZ direction, the shear ultimate strength and shear modulus of the bottom tended to be high as in the XY direction. The shear ultimate strength increased by about 9.3%

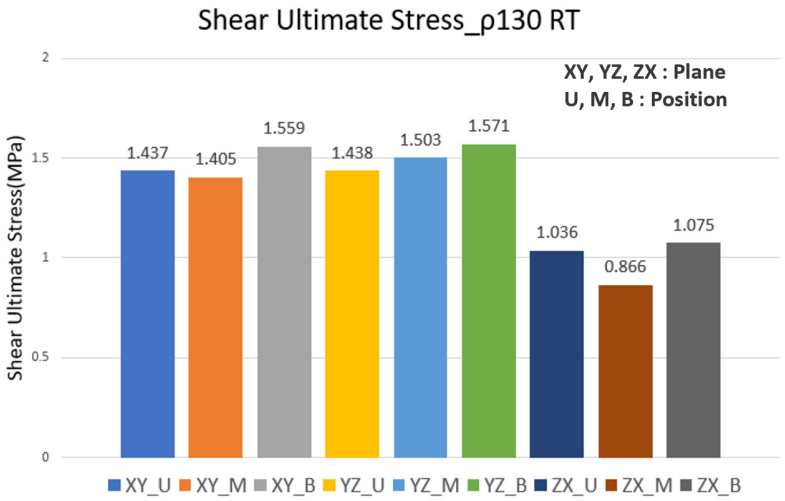

Fig. 21 Ultimate shear ultimate strength of R-PUF by stacking position and coordinate plane for an R-PUF density of 130 kg/m^3 at room temperature

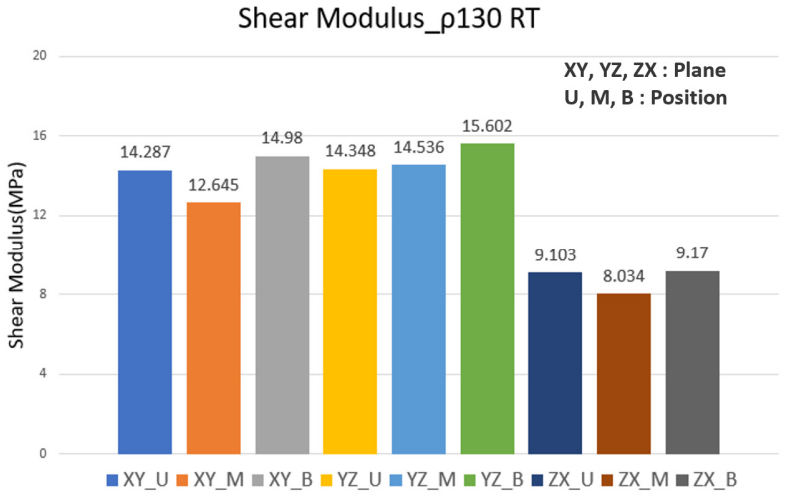

Fig. 22 Shear modulus of R-PUF by stacking position and coordinate plane for an R-PUF density of 130 kg/m^3 at room temperature

Table 6 R-PUF shear test results

Material (Specified density)	Temperature (°C)	Ultimate shear strength (MPa)[1]			Shear modulus (MPa)[1]		
		On the XY plane	On the YZ plane	On the ZX plane	On the XY plane	On the YZ plane	On the ZX plane
R-PUF (130 kg/m^3)	20	1.405 (0.041)	1.503 (0.011)	0.866 (0.039)	12.645 (1.442)	14.536 (0.336)	8.034 (0.164)
	-20	1.324 (0.059)	1.438 (0.099)	1.037 (0.076)	14.816 (0.134)	15.342 (0.295)	9.371 (0.545)
	-70	1.247 (0.045)	1.399 (0.032)	0.896 (0.040)	15.143 (0.287)	15.591 (0.480)	10.762 (0.589)
	-120	1.084 (0.256)	1.494 (0.026)	0.819 (0.009)	13.939 (1.351)	15.847 (0.201)	11.611 (0.705)
	-170	1.348 (0.073)	1.148 (0.005)	0.756 (0.013)	16.675 (0.347)	16.633 (0.031)	12.579 (0.548)

[1] Values within the brackets denote the standard deviation of the corresponding ultimate shear strength/shear modulus.

compared to the upper and 4.5% compared to the middle. The shear modulus increased by about 4.2% compared to the upper and 8.7% compared to the middle.

In the case of the ZX-direction specimen, the shear ultimate strength and shear modulus of the bottom tended to be high. The shear ultimate strength increased by about 3.8% compared to the upper and 24.1% higher than that of the middle. The shear modulus increased by 0.7% compared to the upper and 14.1% compared to the middle.

Also, there were differences in shear ultimate strength and shear modulus depending on the foaming direction.

In the case of the upper part, the shear ultimate strength and shear modulus in the ZX direction tended to be low. The shear ultimate strength decreased by 27.9% compared to the XY direction and decreased by 28% compared to the YZ direction. The shear modulus decreased by 27.9% compared to the XY direction and decreased by 28% compared to the YZ direction.

In the case of the middle part, the shear ultimate strength and shear modulus in the ZX direction tended to be low. Shear ultimate strength decreased by 38.4% compared to the XY direction and 42.4% compared to the YZ direction. The shear modulus was decreased by 36.5% compared to the XY direction and 44.7% compared to the YZ direction.

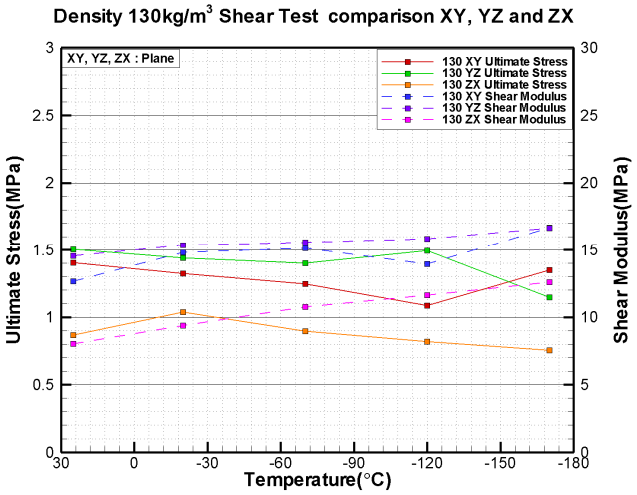

Fig. 23 Density 130 kg/m^3 shear test comparison XY, YZ and ZX

In the case of the bottom part, the shear ultimate strength and shear modulus in the ZX direction tended to be low. Shear ultimate strength decreased by 31.1% compared to the XY direction and 31.6% compared to the YZ direction. The shear modulus was decreased by 38.8% compared to the XY direction and 41.2% compared to the YZ direction.

As shown in Table 6 and Fig. 23, the shear ultimate strength and shear modulus tend to increase as the temperature decreases, and then decrease again after a certain temperature. However, in the case of the ZX-direction specimen, it shows a peculiar tendency to increase rapidly at -20°C and then decrease rapidly again. The standard deviation of all data can be found in Table 6.

5. Conclusions

In this study, compression, tensile, and shear tests were performed on R-PUF, a cryogenic insulation material. The compression test was performed at a test speed of 5 mm/min by dividing by angular density using a 100 × 100 × 50 hexahedral specimen. In the case of room temperature conditions, the tests were performed by dividing the foaming positions (upper, middle, and bottom) by direction. In addition, both shear and tensile tests were compared and evaluated under the same conditions as the aforementioned compression tests. Through each test of the R-PUF material, the static properties of the material were confirmed.

Notably, in the Z direction (amongs the X, Y, and Z directions of the chosen coordinate system), the ultimate tensile strength and tensile Young's modulus of R-PUF decreased by 53.16 and 17.93 % and 52.07 and 16.06 % compared to the X and Y directions, respectively. These decreases appeared to be a characteristic of the manufacturing of R-PUF. So, similar to plywood, R-PUF also had orthotropic properties.

In this study, compression, tensile, and shear tests were performed on R-PUF, a cryogenic insulation material.

As shown in Tables 8 and 9, from the viewpoint of the foaming position, the existing prediction predicted that the density and ultimate tensile strength would increase in proportion, but the test results were different. It was confirmed that the density of the specimen in the upper position was 4.72% higher than that of the specimen in the

Table 7 Tensile test result X, Y and Z comparison

Result	X direction		Y direction		Z direction	
Ultimate tensile strength (MPa)	Upper	2.978	Upper	2.853	Upper	1.350
	Middle	3.141	Middle	3.048	Middle	1.861
	Bottom	3.603	Bottom	3.600	Bottom	1.343
	Average	3.241	Average	3.167	Average	1.518
Tensile modulus (MPa)	Upper	36.008	Upper	34.483	Upper	20.240
	Middle	36.045	Middle	35.092	Middle	51.183
	Bottom	41.682	Bottom	41.629	Bottom	21.914
	Average	37.912	Average	37.068	Average	31.112

Table 8 Density value Upper, Middle and Bottom comparison

	Upper position		Middle position		Bottom position	
Density (kg/m^3)	X direction	123.89	X direction	119.89	X direction	128.36
	Y direction	127.40	Y direction	121.00	Y direction	128.67
	Z direction	128.83	Z direction	122.09	Z direction	130.71
	Average	126.71	Average	120.99	Average	129.25

Table 9 Tensile test result upper, middle and bottom comparison

	Upper position		Middle position		Bottom position	
Ultimate tensile strength (MPa)	X direction	2.978	X direction	3.141	X direction	3.603
	Y direction	2.853	Y direction	3.048	Y direction	3.600
	Z direction	1.350	Z direction	1.861	Z direction	1.343
	Average	2.394	Average	2.683	Average	2.849

Table 10 Comp test result X, Y and Z comparison

Result	X direction		Y direction		Z direction	
Ultimate compressive strength (MPa)	Upper	1.712	Upper	1.818	Upper	1.467
	Middle	1.702	Middle	1.687	Middle	1.918
	Bottom	2.005	Bottom	1.918	Bottom	1.465
	Average	1.806	Average	1.808	Average	1.617
Comp. modulus (MPa)	Upper	30.336	Upper	55.974	Upper	48.69
	Middle	30.449	Middle	50.897	Middle	47.69
	Bottom	40.172	Bottom	57.816	Bottom	51.664
	Average	33.652	Average	54.900	Average	49.348

middle position, but the ultimate tensile strength value was 10.80% lower. This can indirectly confirm that there are factors other than density that affect ultimate tensile strength.

As can be seen from Figs. 13−15, the tensile test result of R-PUF had a large change according to the temperatureFurther, the ultimate tensile strength for all densities of R-PUF tended to increase up to -70°C but decreased from -120°C. However, the tensile Young's modulus continued to increase with decreasing temperature. So, curing occurred in R-PUF under a varying temperature.

In the compression test of R-PUF, the ultimate compressive strength of R-PUF in the Z direction was 10.50 and 10. 57% lower than that in the X and Y directions, respectively. This lower ultimate compressive strength was also seen as a result of the orthotropic properties of R-PUF. Here, the compressive modulus tends to be different from the ultimate compressive strength, and the compressive modulus of the X direction specimen tends to be 38.70% lower than that of the Y direction specimen, and 31.81% lower than the Z direction specimen

As shown in Tables 8 and 11, as mentioned earlier, the ultimate compressive strength was expected to increase in proportion to the density, but in the compression test, similar to the tensile test, the density of the specimen in the upper position was 4.72% higher than that of the specimen in the middle position, but it was confirmed that the ultimate compressive strength value was 5.84% lower.

Table 11 Comp. test result Upper, Middle and Bottom comparison

	Upper position		Middle position		Bottom position	
Ultimate compressive strength (MPa)	X direction	1.712	X direction	1.702	X direction	2.005
	Y direction	1.818	Y direction	1.687	Y direction	1.918
	Z direction	1.467	Z direction	1.918	Z direction	1.465
	Average	1.670	Average	1.769	Average	1.796

Table 12 Shear test result XY, YZ and ZX comparison

Result	XY plane		YZ plane		ZX plane	
Ultimate shear strength (MPa)	Upper	1.437	Upper	1.438	Upper	1.036
	Middle	1.405	Middle	1.503	Middle	0.866
	Bottom	1.559	Bottom	1.571	Bottom	1.075
	Average	1.467	Average	1.504	Average	0.992
Shear modulus (MPa)	Upper	14.287	Upper	14.348	Upper	9.103
	Middle	12.645	Middle	14.536	Middle	8.034
	Bottom	14.980	Bottom	15.602	Bottom	9.170
	Average	13.971	Average	14.830	Average	8.769

Table 13 Shear test result upper, middle and bottom comparison

Result	Upper position		Middle position		Bottom position	
Ultimate shear strength (MPa)	XY Plane	1.437	XY Plane	1.405	XY Plane	1.559
	YZ Plane	1.438	YZ Plane	1.503	YZ Plane	1.571
	ZX Plane	1.036	ZX Plane	0.866	ZX Plane	1.075
	Average	1.304	Average	1.258	Average	1.402
Shear modulus (MPa)	XY Plane	14.287	XY Plane	12.645	XY Plane	14.980
	YZ Plane	14.348	YZ Plane	14.536	YZ Plane	15.602
	ZX Plane	9.103	ZX Plane	8.034	ZX Plane	9.170
	Average	12.579	Average	11.738	Average	13.251

Additionally, the R-PUF compression test results showed a large change in the ultimate compressive strength and compressive Young's modulus of R-PUF according to the temperature change. As shown in Figs. 18–20, it was confirmed that the ultimate compressive strength and compressive modulus increased as the temperature decreased. In the case of a density of 130 kg/m^3, the ultimate compressive strength and compressive modulus increased by 98.52% and 78.12%, respectively, at -170°C compared to 20°C. In the case of density of 170 kg/m^3, ultimate compressive strength and compressive modulus increased by 140.42% and 122.79% respectively at -170°C compared to 20°C. At a density of 210 kg/m^3, the ultimate compressive strength and compressive modulus increased by 136.52% and 191.51%, respectively, at -170°C compared to 20°C This correlation appeared to be a result of the hardening phenomenon of R-PUF.

Meanwhile, in the R-PUF shear test, the ultimate shear strength and shear modulus of R-PUF on the ZX plane were the lowest from the viewpoint of the foaming direction. It was 32.36% and 37.23% lower than those on the XY and YZ planes by 32.36 and 37.23% and 34.02 and 40.86 %, respectively. These lower values on the ZX plane indicated the weakness of R-PUF that came from R-PUF manufacturing characteristics.

As shown in Tables 8 and 13, The results of the shear test confirmed that the density had the greatest effect on the results of the shear test, as expected. The density of the highest bottom compared to the middle with the lowest density was 6.83%, ultimate shear strength was 11.45% higher, and shear modulus was 12.89% higher. As the density increased, ultimate shear strength and shear modulus were increased.

As shown in Fig. 23, it can be seen that the shear test results according to the temperature do not have a large effect on the ultimate shear strength of R-PUF was largely affected by temperature, but the shear modulus was not. So, these effects appeared to be a phenomenon caused by the curing of R-PUF.

Overall, the density was the factor having the greatest influence on the ultimate strength and Young's modulus of R-PUF, but there were likely other factors of such a great influence as well. Further, it was confirmed that the Z direction and the ZX plane were the weakest direction and plane of R-PUF, respectively. Finally, the higher the density of R-PUF, the greater the hardening phenomenon of R-PUF according to the temperature drop.

Conflict of Interest

The author declare that they have no conflict of interests.

Funding

This research was supported by the research funds of Mokpo National University in 2020.

References

Ahn, J.H., Kim, J.H., Kim, J.D., Park, S.K., Park, K.H., Byun, J.S., & Lee, J.M. (2018). Development and Mechanical and Thermal Performance Evaluation of Polyurethane foam Composites Reinforced with Glass Bubbles. Journal of the Korean Society of Marine Engineering, 42(9), 708−714. http://doi.org/10.5916/jkosme.2018.42.9.708

Denay, A.G., Castagnet, S., Roy, A., Alise1, G., & Thenard, N. (2013). Compression Behavior of Glass-fiber-reinforced and Pure Polyurethane Foams at Negative Temperatures Down to Cryogenic Ones. Journal of Cellular Plastics, 49(3), 209−222. https://doi.org/10.1177/0021955X13477672

Jang, C.W., Shim, C.S., Song, H.C., & Song, C.Y. (2013). Study on Cryogenic Behavior of Reinforced Polyurethane Foam for Membrane Type LNG Carrier. Journal of Ocean Engineering and Technology, 27(1), 74−79. https://doi.org/10.5574/KSOE.2013.27.1.074

Han, D.S., Park, I.B., Kim, M.H., Noh, B.J., Kim, W.S., & Lee, J.M. (2010). The Effects of Glass Fiber Reinforcement on the Mechanical Behavior of Polyurethane Foam. Journal of Mechanical Science and Technology, 24, 263−266. https://doi.org/10.1007/s12206-009-1136-3

Kim, M.S., Kim, J.H., Kim, S.K., & Lee, J.M. (2019a). Effect of Repetitive Impacts on the Mechanical Behavior of Glass Fiber-reinforced Polyurethane Foam. Journal of Ocean Engineering and Technology 33(1), 85−91. https://doi.org/10.26748/KSOE.2018.068

Kim, J.Y., Kim, J.D., & Lee, J.M. (2019b). Mechanical and Thermal Characteristics of Polyurethane Foam with Tow Different Reinforcements and the Effects of Ultrasonic Dispersion in Manufacturing. Journal of the Society of Naval Architects of Korea, 56(6), 515−522. http://doi.org/10.3744/SNAK.2019.56.6.515

Lee, C.S., Kim, M.S., Park, S.B., Kim, J.H., Bang, C.S., & Lee, J.M. (2015). A Temperature- and Strain-rate-dependent Isotropic Elasto-viscoplastic Model for Glass-fiber-reinforced Polyurethane Foam. Materials and Design, 84, 163−172. https://doi.org/10.1016/j.matdes.2015.06.086

Oh, J.H., Bea, J.H., & Lee, J.M. (2018). The Effects of Kevlar Pulp on Polyurethane Foam for Cryogenic Temperature. Journal of the Society of Naval Architects of Korea, 55(6), 514−520. https://doi.org/10.3744/SNAK.2018.55.6.514

Park, S.B., Kim, J.H., & Lee, J.M. (2014). Comparative Study on Mechanical Behavior of Low Temperature Characteristics of Polymeric Foams for Ships and Offshore Structures. Journal of the Society of Naval Architects of Korea, 51(6), 495−502. https://doi.org/10.3744/SNAK.2014.51.6.495

Park, S.B., Lee, C.S., Choi, S.W., Kim, J.H., Bang, C.S., & Lee, J.M. (2016). Polymeric Foams for Cryogenic Temperature Application: Temperature Range for Non-recovery and Brittle-fracture of Microstructure. Composite Structures, 136, 258−269. https://doi.org/10.1016/j.compstruct.2015.10.002

Author ORCIDs

Author name	ORCID
Song, Ha-Cheol	0000-0002-6233-3826